

Research Article

Optical and Structural Properties of Silicon Nanocrystals Embedded in SiO_x Matrix Obtained by HWCVD

A. Coyopol, G. García-Salgado, T. Díaz-Becerril, H. Juárez, E. Rosendo, R. López, M. Pacio, J. A. Luna-López, and J. Carrillo-López

CIDS-ICUAP, Benemérita Universidad Autónoma de Puebla, 14 sur y Avenida San Claudio, Edif. 137, 72570 Puebla, PUE, Mexico

Correspondence should be addressed to A. Coyopol, acoyopol@gmail.com

Received 24 February 2012; Accepted 22 May 2012

Academic Editor: Grégory Guisbiers

Copyright © 2012 A. Coyopol et al. This is an open access article distributed under the Creative Commons Attribution License, which permits unrestricted use, distribution, and reproduction in any medium, provided the original work is properly cited.

The interest in developing optoelectronic devices integrated in the same silicon chip has motivated the study of Silicon nanocrystals (Si-ncs) embedded in SiO_x (nonstoichiometric silicon oxides) films. In this work, Si-ncs in SiO_x films were obtained by Hot Wire Chemical Vapor Deposition (HWCVD) at 800, 900, and 1000°C. The vibration modes of SiO_x films were determined by FTIR measurements. Additionally, FTIR and EDAX were related to get the proper composition of the films. Micro-Raman studies in the microstructure of SiO_x films reveal a transition from amorphous-to-nanocrystalline phase when the growth temperature increases; thus, Si-ncs are detected. Photoluminescence (PL) measurement shows a broad emission from 400 to 1100 nm. This emission was related with both Si-ncs and interfacial defects present in SiO_x films. The existence of Si-ncs between 3 and 6 nm was confirmed by HRTEM.

1. Introduction

It is known that bulk silicon is the dominant semiconductor material in microelectronics industry; however, limited to the development of optoelectronic devices due to be an indirect band-gap semiconductor.

Since the observation of intense photoluminescence from porous silicon (PS) at room temperature [1], properties of low dimensional silicon quantum structures have been a subject of extensive investigations [2, 3]. Silicon-based nanostructures have been published so far with the majority devoted to the optical properties of nanocrystalline silicon embedded in SiO_x films. Although the phenomenon of emission produced in the SiO_x films has not yet been satisfactorily explained, there are different theories about the origin of the PL, such as quantum confinement [4], siloxanes (Si₆O₃H₆) [5], surface defects by bonds (SiH₂)_x [6], and interfacial defects in networks Si/SiO_x [7–9]. The widely accepted theory is the Quantum confinement; this theory says that Si-ncs produce a change in the bands structure by increasing the width of the band-gap crystalline silicon and making the direct transitions possible.

SiO_x films are obtained by different growth techniques such as: Sputtering [10], ion-implantation [11], catalytic-CVD (Cat-CVD) [12], Plasma Enhanced Chemical Vapor Deposition (PECVD) [13], and HWCVD [14]. The SiO_x films grown by different techniques have interesting characteristics due to presence of large number of Si–Si bonds, which are subsequently ordered and, therefore, they can be considered as Si clusters embedded in SiO_x matrix. In most cases the Si clusters can be crystallized only under high temperature annealing [15, 16] to form Si-ncs. However, it is known that thermal annealing increases the technological cost because it requires both high temperatures and long annealing times on inert atmospheres.

In this paper, optical and structural properties of SiO_x films are reported, we demonstrated the presence of Si-ncs in SiO_x films grown by HWCVD technique without using subsequent thermal process. The SiO_x films were characterized by FTIR (Fourier Transform Infrared), EDAX (Energy-Dispersive X-Ray Spectroscopy), Micro-Raman, PL, and HRTEM (High Resolution Transmission Electron Microscopy) techniques.

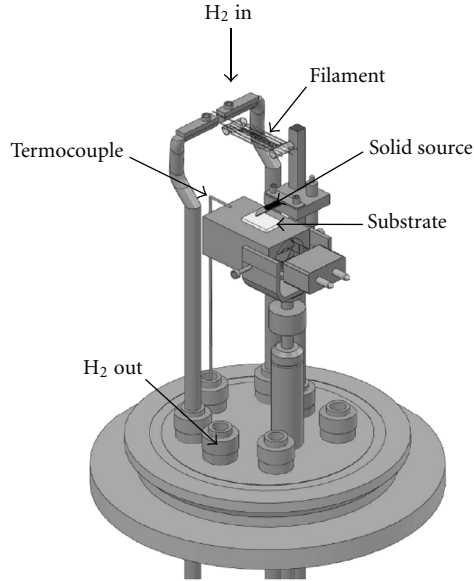


FIGURE 1: Detailed diagram of the HWCVD system.

2. Experimental Details

SiO_x films were synthesized in an HWCVD reactor at temperatures of 800, 900, and 1000°C, using a solid source of PS and atomic hydrogen.

The HWCVD technique involves the dissociation of molecular hydrogen using a hot filament at about 2000°C. To reach this temperature, measurements of applied voltage versus resistivity of tungsten filament are performed to obtain the voltage necessary (84.6 V) and keep a temperature of 2000°C during the process. The growth of SiO_x films by HWCVD is as follows: molecular hydrogen is introduced through the chamber with a constant flow of 20 sccm. A tungsten filament heated to 2000°C produces atomic hydrogen which reacts with a solid source of porous silicon. Gas precursors of Silane (SiH_4) and silicon monoxide (SiO) are generated and transported to the substrate forming SiO_x films.

The HWCVD technique used in this work, differs from conventional Cat-CVD; which consist in the thermal decomposition of reactant gases at the surface of a hot-filament heated at temperatures in the range of 1500–2000°C [12]. HWCVD produces its gaseous precursors from the interaction of atomic hydrogen and a solid source of PS or quartz. This peculiarity of the HWCVD technique makes it a potential alternative for the growth of SiO_x films.

The filament-source distance was kept constant at 3 mm, while the filament-substrate distance was 10 mm, 11.5 mm and 13.2 mm, to obtain a deposition temperature of 1000, 900, and 800°C, respectively. The growth time was 10 minutes for each sample. A detailed diagram of the HWCVD system is shown in Figure 1.

For the different optical and structural characterizations, SiO_x films were deposited on two types of substrates. Quartz was used for characterization of PL, HRTEM, Micro-Raman,

TABLE 1: Main bonds of the SiO_x films grown at different temperatures.

Vibration type	Vibration of SiO_x obtained in this work (cm^{-1})			Reference
	1000°C	900°C	800°C	
Si–O–Si rocking	450	452	448	[17]
Si–O–Si bending	800	801	798	[17]
Si–O–Si stretching	1080	1077	1066	[18]
SiH bending	878	880	881	[19]
SiH wagging	660	670	674	[20]

and silicon (n-type (100)) for FTIR and EDAX measurements. The substrates of silicon were carefully cleaned with an MOS standard cleaning process and the native oxide was removed with an HF buffer solution before being introduced into the reactor. PS layers used as solid sources were prepared by anodic etching a p-type Si (100) wafer, resistivity $\sim 0.04 \Omega\text{-cm}$, in a 40% HF and ethanol electrolyte (1:2).

FTIR absorbance measurements were performed on a Bruker Vector 22 spectrometer in the range 400 to 4000 cm^{-1} . The composition of the films was determined by EDAX and FTIR by using the relation $\text{SiO}_x \rightarrow a\text{Si} + b\text{SiO}_x$, where a , b are called the silicon separation coefficient and silicon oxide matrix coefficient, respectively.

Micro-Raman measurements were performed at room temperature by using a He-Ne laser (632.8 nm). A laser with a wavelength of 405 nm and 40 mW of power was used to excite the sample in PL measurements; the range detected by monochromator was from 400 to 1100 nm. Finally, a HRTEM FEI Tecnai F30 STWIN G2 was used to observe the presence of Si-ncs in SiO_x films.

3. Results and Discussions

Infrared absorption spectra of SiO_x films grown at 800, 900, and 1000°C on silicon substrates are shown in Figure 2(a). Characteristics bands of SiO_2 have been reported around 460, 800, and 1080 cm^{-1} . The main absorption peak around of 1080 cm^{-1} is associated with the Si–O–Si stretching mode, while those at 800 and 460 cm^{-1} correspond to bending and rocking modes, respectively. Results of infrared spectroscopy of films grown at different temperatures are shown in Table 1, where absorption peaks, their identifications, and references are recorded.

We observe that as the substrate temperature decreases (Table 1), the wavenumber of the main peak shifts from 1080 cm^{-1} (SiO_x , $x = 2$) to 1066 cm^{-1} (SiO_x , $x < 2$). According to the FTIR analysis of SiO_x films produced by PECVD [17], the silicon atoms have a higher probability of having one or more silicon atom neighbors, when $x < 2$.

In this way, it is likely that two phases coexist in the films; the silicon oxide (SiO_x) phase and another due to silicon bonds [21]. The shift observed in the stretching peak indicates phase separation in the films according to

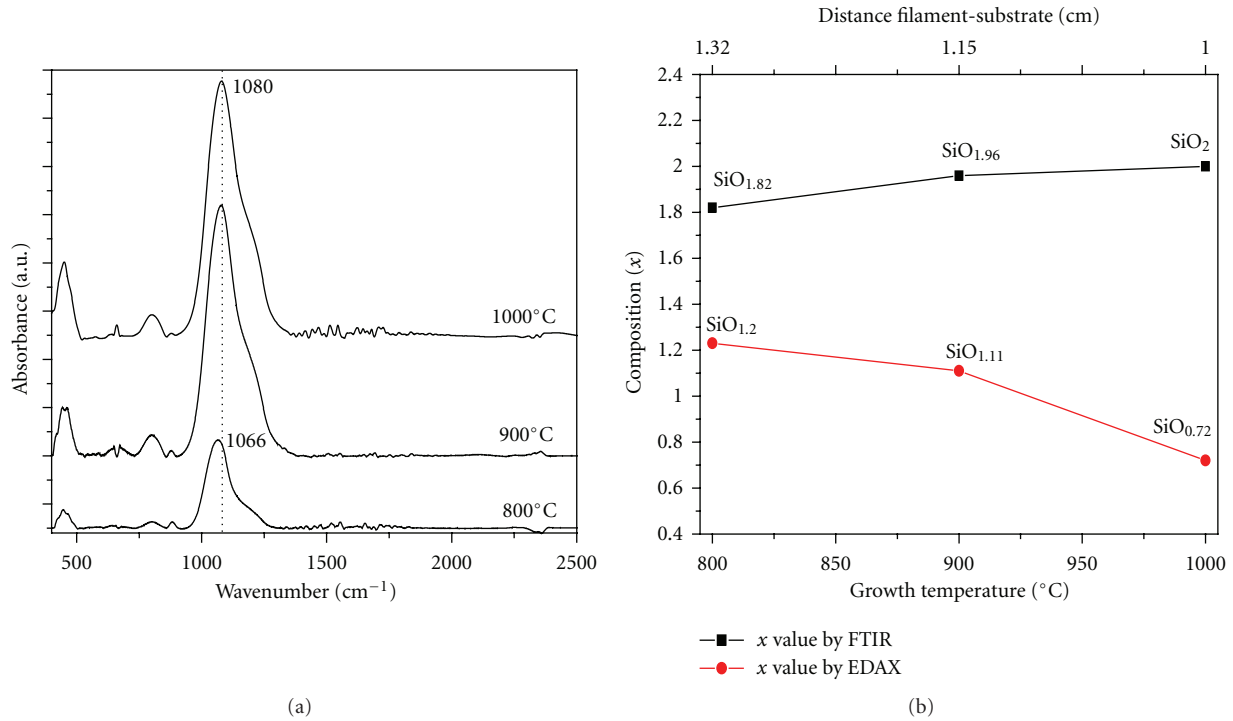


FIGURE 2: (a) Spectra FTIR of SiO_x films grown at different temperatures, (b) graphics composition of the silicon oxide phase obtained by FTIR and of the whole film found by EDAX.

TABLE 2: Composition data of the silicon oxide phase by FTIR and composition data of the whole film found by EDAX.

Growth temperature (°C)	Composition by EDAX	Composition of SiO _x phase by FTIR	Coefficient	
	<i>x</i>	<i>x</i>	<i>a</i>	<i>b</i>
800	1.2	1.82	0.34	0.65
900	1.11	1.96	0.43	0.56
1000	0.72	2	0.64	0.36

the variation in the x value. By FTIR spectroscopy the x value of the silicon oxide phase could be calculated by $x = (\nu - 918)/81$ [17], where ν is the shift Si–O–Si stretching frequency. From this result, we find the x value of the silicon oxide phase; $x = 2, 1.96,$ and 1.82 for the samples grown at 1000, 900, and 800°C respectively, these data are shown in Table 2. In general, we observe that the x value obtained by FTIR is close to silicon dioxide (SiO₂) stoichiometry value.

In order to determine the composition of the whole film, qualitative studies in the SiO_x films were done by EDAX. It was found a composition ratio ($x = O/Si$) of 1.23, 1.17, and 0.72 for samples grown at 800, 900, and 1000°C respectively (Table 2). It is important to mention that the EDAX results are for the whole film and the FTIR outcomes gives the composition of the silicon oxide phase only. The actual Si clusters and Si and oxygen of silicon oxide matrix were detected by EDAX measurement.

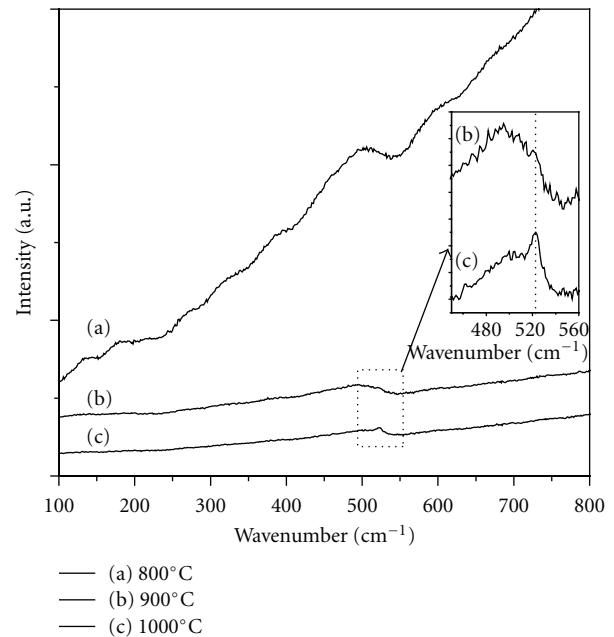


FIGURE 3: Micro-Raman of the films growth at 800, 900, and 1000°C.

EDAX studies reveal a high concentration of silicon as the filament-substrate distance decrease. The value of x decreases indicating an increase in the content of silicon as shown in Figure 2(b), where we plot the composition values of the silicon oxide phase obtained by FTIR and the composition of the whole film found by EDAX.

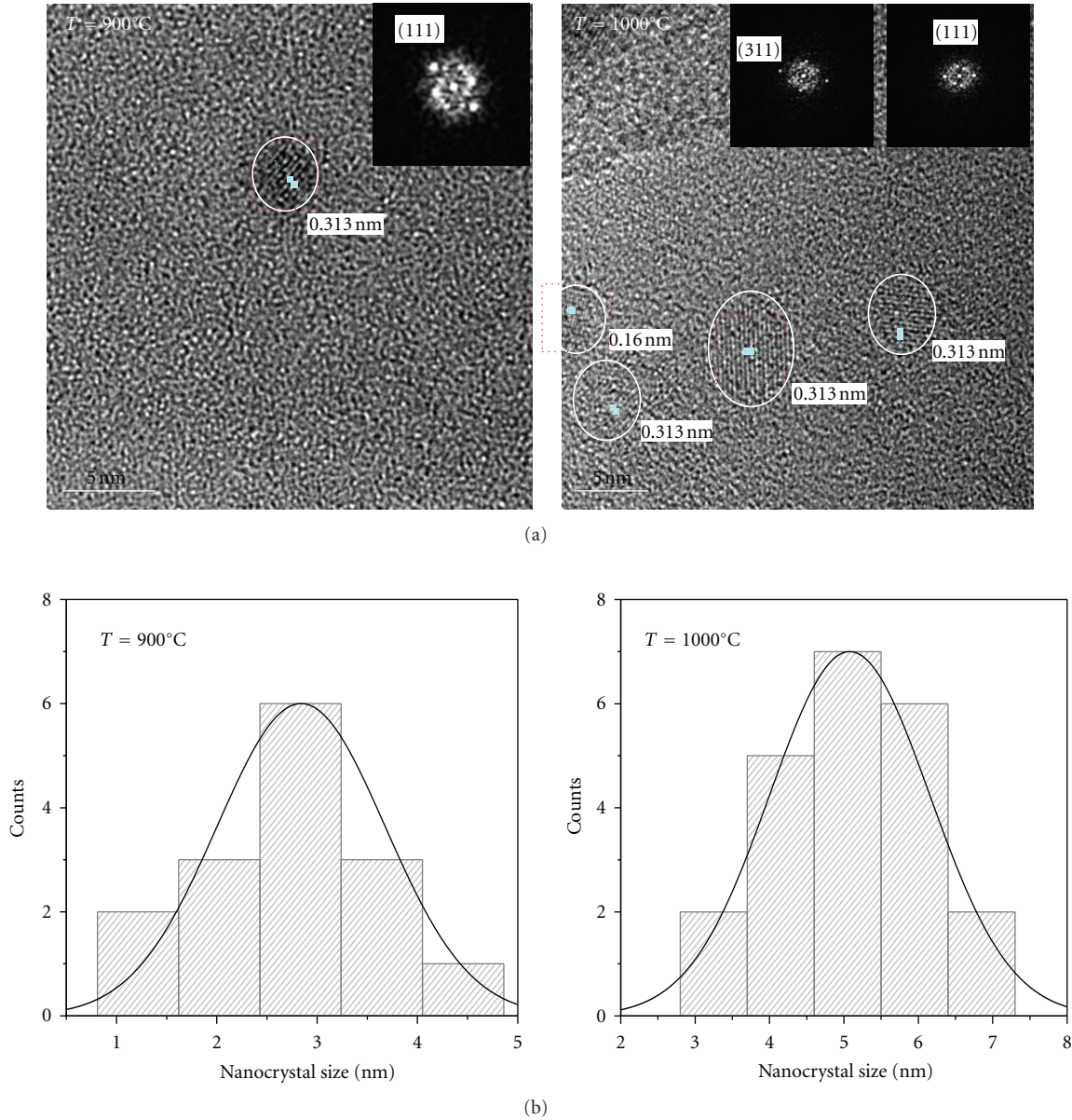


FIGURE 4: (a) HRTEM images of the samples grown at 900°C and 1000°C, (b) histograms corresponding to the samples grown at 900 and 1000°C.

Thus, it is suggested to have a mixture of two phases, using the relationship $\text{SiO}_x = a\text{Si} + b\text{SiO}_x$ for the composition of both silicon and silicon dioxide phases, we obtain coefficients a , b , which are called the silicon separation coefficient and silicon oxide matrix coefficient, respectively [22]. Coefficients a , b are shown in Table 2. We can deduce that the relatively high growth temperatures (800–1000°C) may induce diffusion of silicon atoms in silicon oxide structure, causing phase separation and the formation of silicon clusters embedded in a matrix of SiO_x . This way, for the film deposited at 800°C, it is gotten a composition of $\text{SiO}_{1.2} \rightarrow 0.34\text{Si} + 0.65\text{SiO}_{1.82}$.

Silicon clusters in amorphous phase or amorphous-nanocrystalline phase are found in SiO_x films. These

amorphous-nanocrystalline phases are detected by micro-Raman measurements. In Figure 3, micro-Raman spectra of the SiO_x films grown at 800, 900, and 1000°C; are presented. The spectrum of the sample grown at 800°C presents two bands around 180 cm^{-1} and 480 cm^{-1} . These bands are related to disorder-activated modes in amorphous silicon [23, 24]. For samples grown at 900 and 1000°C: a reduction in the amorphous bands takes place and a small peak appears at 521.84 cm^{-1} [25]. The peak centered around 521.84 cm^{-1} has a full width at half maximum (FWHM) of 6.58 cm^{-1} and 9.54 cm^{-1} for samples grown at 900 and 1000°C respectively; these peak shows the presence of Si-ncs, so the increase in substrate temperature helps to promote the phase of Si-ncs. This effect could be explained as follow:

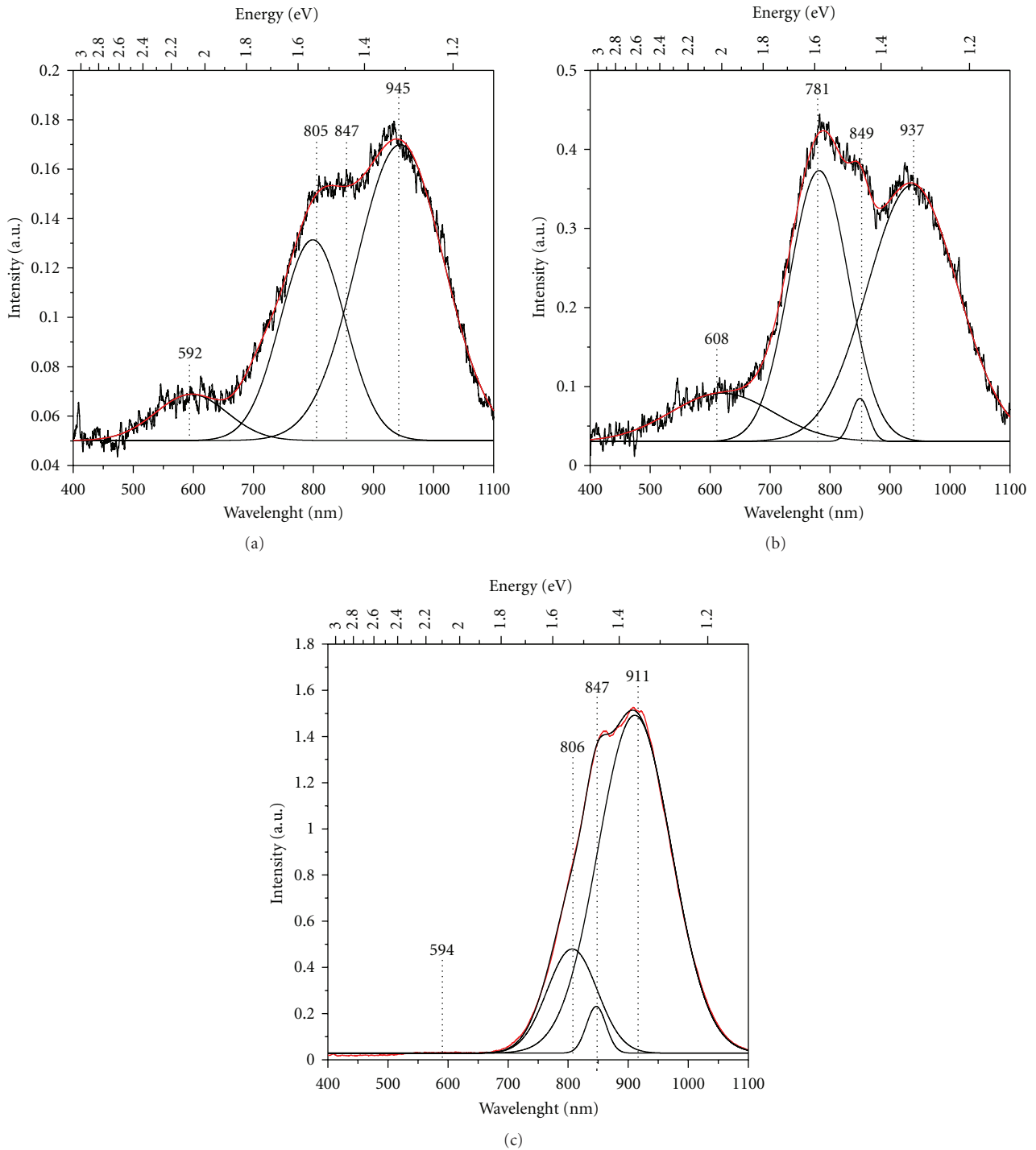


FIGURE 5: PL of SiO_x films grown at (a) 800°C , (b) 900°C , and (c) 1000°C .

we assume that high temperature induces diffusion of silicon to the formation of silicon clusters embedded in a matrix SiO_x , so while the process is taking place, exist an in situ annealing caused by the high growth temperature. Thus, when growth temperature significantly increases the clusters start to crystallize to form the Si-ncs.

It has been reported that crystallization of silicon clusters on annealing processes takes place at high temperatures

($1000\text{--}1300^\circ\text{C}$) [15, 16]. In the highlights of these SiO_x films obtained by HWCVD, the crystallization of silicon clusters was obtained at growth temperatures of 900°C as suggested the micro-Raman results.

Figure 4(a), shows the HRTEM images for samples grown at 900°C and 1000°C . HRTEM images confirmed the existence of Si-ncs with a mean square value about 5 nm. The average size found for sample grown at 900°C was 3 nm and

for sample grown at 1000°C varied between 3 and 6 nm as shown the histograms in Figure 4(b).

Amorphous silicon clusters detected by Micro-Raman cannot be observed by HRTEM, only silicon crystals of nanometer size are observed. For SiO_x films grown at 800°C, we suggest that the growth temperature is not enough to achieve crystallization in the silicon clusters. For films grown at 900 and 1000°C the silicon clusters begins to crystallize, suggesting the formation of a nanocrystalline core in silicon clusters. Thus, we proposed that silicon clusters consist in Si-ncs (nanocrystalline cores) surrounded by an amorphous silicon shell, where the size of the Si-ncs depends of the growth temperature. The formation of silicon clusters is carried out entirely by diffusion mechanism of silicon in SiO₂ [26]. This diffusion is dependent on growth temperature, so the higher growth temperature the diffusion of silicon atoms is higher and clusters should therefore be larger.

Nanocrystal lattice spacing in HRTEM images was estimated using the digital micrograph 3.7 software. Interplanar distances of 0.313, 0.16 nm were measured; these distances correspond to (111) and (311) planes of silicon [27]; respectively. Fast Fourier transform (FFT) of the selected area in the HRTEM images (red squares) produces a diffractogram, in which it was possible to determine the structure of the crystals formed (upper right side in Figure 4(a)).

PL measurements were performed at room temperature in a range of emission from 400 to 1100 nm. SiO_x films grown at 800, 900 and 1000°C show a broad PL emission from 450 to 1100 nm (Figure 5). Peaks around 600, 800, 847 and 930 nm are observed after applying the appropriate deconvolution. As is well known, several hypotheses have been proposed to explain the PL origin of Si-ncs in SiO_x films. Quantum confinement (QC) and the model that relates the PL with the presence of defects in the SiO₂/Si-ncs matrix and/or interface [7–9] are two of the main mechanisms responsible for efficient light emission from nano-sized structures based in silicon. In the SiO_x films grown by HWCVD, some interface defects may exist: the one between crystalline core and amorphous silicon shell and the one between silicon amorphous shell and the surrounding matrix (SiO_x).

Si-ncs observed by HRTEM are sufficiently small to observe QC effect. PL peaks at 600, 800, and 847 nm are generally attributed to the presence of silicon nanoparticles [28, 29]. However this does not exclude the possibility that defects such as Neutral Charged Oxygen Vacancies (NOV) (Si–Si bonds), No Bridging Oxygen Hole Center (NBOHC), positively charged oxygen vacancies (E-centers), interstitial oxygen molecules, and peroxide radicals [30–32] may be responsible for the PL, because the emissions are located in the same range of wavelengths.

The band emission in the infrared region with peak main at 930 nm is related to defects, this range of emissions is not allowed for emissions due to Si-ncs because there is a reduced likelihood of QC. There is a linear relation between the PL peak energy and the reciprocal of the square of crystallite size [33], Thus for an peak energy around 930 nm, it is likely estimated by the ratio $d^{-1.39}$ [31, 33] a diameter of the nanocrystal, $d > 5$ nm, which do not agree to the Bohr radius

of the bulk silicon (5 nm) [34], which is necessary for the quantum confinement.

We propose that both effects must be responsible for the phenomenon of PL; however a thorough study is needed to support these assumptions.

4. Conclusion

Silicon nanocrystals in a SiO_x matrix were synthesized by the HWCVD technique. Characteristic peaks of SiO₂ as well as peaks due to the presence of hydrogen are detected by FTIR. Using EDAX and FTIR characterization was obtained the composition of the SiO_x films, this composition is a mixture of two phases; a phase due to the silicon and the other phase due to silicon oxide. The crystallization temperature of silicon clusters occurs around 900 and 1000°C, this crystallization results in the formation of Si-ncs. It is proposed that the Si-ncs observed by HRTEM are surrounded by amorphous silicon. It is likely that the Si-ncs observed by HRTEM between 3 and 6 nm are responsible of the photoluminescence in films, however the Si-ncs should be surrounded by defects which cause part of the emission, so we proposed that both effects are producing the emission in SiO_x films.

Acknowledgments

A. Coyopol acknowledges the support received from CONACYT and ICUAP-BUAP. The authors would like to thank the technicians from IPYCIT HRTEM measurements performed.

References

- [1] L. T. Canham, “Silicon quantum wire array fabrication by electrochemical and chemical dissolution of wafers,” *Applied Physics Letters*, vol. 57, no. 10, article 1046, 3 pages, 1990.
- [2] P. M. Anbarasan, P. Senthilkumar, S. Manimegalai et al., “Spectral and morphological studies of nanocrystalline silicon thin films synthesized by PECVD for solar cells,” *Silicon*, vol. 2, no. 1, pp. 7–17, 2010.
- [3] C. D. Presti, A. Irrera, G. Franzó et al., “Photonic-crystal silicon-nanocluster light-emitting device,” *Applied Physics Letters*, vol. 88, no. 3, Article ID 033501, 3 pages, 2006.
- [4] D. J. Lockwood, “Optical properties of porous silicon,” *Solid State Communications*, vol. 92, no. 1-2, pp. 101–112, 1994.
- [5] M. S. Brandt, H. D. Fuchs, M. Stutzmann, J. Weber, and M. Cardona, “The origin of visible luminescence from “porous silicon”: a new interpretation,” *Solid State Communications*, vol. 81, no. 4, pp. 307–312, 1992.
- [6] J. F. Du, T. Wan, and B. Zhou, “Visible light emission at room temperature from PECVD a-Si:H:O,” *Journal of Non-Crystalline Solids*, vol. 164–166, no. 2, pp. 945–948, 1993.
- [7] H. Z. Song and X. M. Bao, “Visible photoluminescence from silicon-ion-implanted SiO₂ film and its multiple mechanisms,” *Physical Review B*, vol. 55, no. 11, pp. 6988–6993, 1997.
- [8] N. Daldosso, M. Luppi, S. Ossicini et al., “Role of the interface region on the optoelectronic properties of silicon nanocrystals embedded in SiO₂,” *Physical Review B*, vol. 68, no. 8, Article ID 085327, 2003.

- [9] H. Z. Song, X. M. Bao, N. S. Li, and J. Y. Zhang, "Relation between electroluminescence and photoluminescence of Si⁺-implanted SiO₂," *Journal of Applied Physics*, vol. 82, no. 8, Article ID 4028, 5 pages, 1997.
- [10] M. Zacharias and P. Streitenberger, "Crystallization of amorphous superlattices in the limit of ultrathin films with oxide interfaces," *Physical Review B*, vol. 62, no. 12, pp. 8391–8396, 2000.
- [11] T. Shimizu-Iwayama, S. Nakao, and K. Saitoh, "Visible photoluminescence in Si⁺-implanted thermal oxide films on crystalline Si," *Applied Physics Letters*, vol. 65, no. 14, pp. 1814–1816, 1994.
- [12] Y. Matsumoto, S. Godavarthi, M. Ortega, V. Sánchez, S. Velumani, and P. S. Mallick, "Size modulation of nanocrystalline silicon embedded in amorphous silicon oxide by Cat-CVD," *Thin Solid Films*, vol. 519, no. 14, pp. 4498–4501, 2011.
- [13] Z. X. Ma, X. B. Liao, J. He et al., "Annealing behaviors of photoluminescence from SiO_x:H," *Journal of Applied Physics*, vol. 83, no. 12, pp. 7934–7939, 1998.
- [14] P. Salazar, F. Chávez, F. Silva-Andrade, A. V. Ilinskii, N. Morales, and R. Peña-Sierra, "Photoluminescence from amorphous silicon oxide films prepared by HFCVD technique," *Modern Physics Letters B*, vol. 15, no. 17–19, pp. 756–759, 2001.
- [15] G. Franzó, M. Miritello, S. Boninelli et al., "Microstructural evolution of SiO_x films and its effect on the luminescence of Si nanoclusters," *Journal of Applied Physics*, vol. 104, no. 9, Article ID 094306, 5 pages, 2008.
- [16] D. Riabinina, C. Durand, J. Margot, M. Chaker, G. A. Botton, and F. Rosei, "Nucleation and growth of Si nanocrystals in an amorphous SiO₂ matrix," *Physical Review B*, vol. 74, no. 7, Article ID 075334, 7 pages, 2006.
- [17] P. G. Pai, S. S. Chao, Y. Takagi et al., "Infrared spectroscopic study of SiO_x films produced by plasma enhanced chemical vapor deposition," *Journal of Vacuum Science & Technology A*, vol. 4, no. 3, pp. 689–694, 1986.
- [18] H. J. Cheong, J. H. Kang, J. K. Kim et al., "Formation of luminescent Si nanocrystals by high-temperature rapid thermal chemical vapor deposition," *Applied Physics Letters*, vol. 83, no. 14, pp. 2922–2924, 2003.
- [19] Y. Fukuda, W. Zhou, K. Furuya, and H. Suzuki, "Photoluminescence change of as-prepared and aged porous silicon with NaOH treatment," *Journal of the Electrochemical Society*, vol. 146, no. 7, pp. 2697–2701, 1999.
- [20] N. Jeyakumaran, B. Natarajan, S. Ramamurthy, and V. Vasu, "Effect of nitrogen on optical properties of porous silicon," *Journal for Bloomers of Research*, vol. 2, no. 2, p. 116, 2010.
- [21] M. Molinari, H. Rinnert, and M. Vergnat, "Visible photoluminescence in amorphous SiO_x thin films prepared by silicon evaporation under a molecular oxygen atmosphere," *Applied Physics Letters*, vol. 82, no. 22, pp. 3877–3879, 2003.
- [22] C.-T. Lee, Y.-F. Chen, and C.-H. Lin, "Phase-separated Si nanoclusters from Si oxide matrix grown by laser-assisted chemical vapor deposition," *Nanotechnology*, vol. 20, no. 2, Article ID 025702, 2009.
- [23] R. Tubino, L. Piseri, and G. Zerbi, "Lattice dynamics and spectroscopic properties by a valence force potential of diamondlike crystals: C, Si, Ge, and Sn," *The Journal of Chemical Physics*, vol. 56, no. 3, pp. 1022–1039, 1972.
- [24] Y. Yang, L. Xu, F. Yang et al., "Enhanced visible photoluminescence from nc-Si/SiO_x films deposited by electron beam evaporation," *Journal of Non-Crystalline Solids*, vol. 356, no. 50–51, pp. 2790–2793, 2010.
- [25] S. Hernández, A. Martínez, P. Pellegrino et al., "Silicon nanocluster crystallization in SiO_x films studied by Raman scattering," *Journal of Applied Physics*, vol. 104, no. 4, Article ID 044304, 5 pages, 2008.
- [26] L. A. Nesbit, "Annealing characteristics of Si-rich SiO₂ films," *Applied Physics Letters*, vol. 46, no. 1, pp. 38–40, 1985.
- [27] W. F. McClune, Ed., *Powder Diffraction File*, International Centre for Diffraction Data, Newtown Square, Pa, USA, 2006.
- [28] X. Y. Chen, Y. F. Lua, L. J. Tang et al., "Annealing and oxidation of silicon oxide films prepared by plasma-enhanced chemical vapor deposition," *Journal of Applied Physics*, vol. 97, no. 1, Article ID 014913, 10 pages, 2005.
- [29] H. Takagi, H. Owada, Y. Yamazaki, A. Ishizaky, and T. Nakagiri, "Quantum size effects on photoluminescence in ultrafine Si particles," *Applied Physics Letters*, vol. 56, no. 24, p. 2379, 1990.
- [30] T. Inokuma, Y. Wakayama, T. Muramoto, R. Aoki, Y. Kurata, and S. Hasegawa, "Optical properties of Si clusters and Si nanocrystallites in high-temperature annealed SiO_x films," *Journal of Applied Physics*, vol. 83, no. 4, pp. 2228–2234, 1998.
- [31] G.-R. Lin, C.-J. Lin, C.-K. Lin et al., "Oxygen defect and Si nanocrystal dependent white-light and near-infrared electroluminescence of Si-implanted and plasma-enhanced chemical-vapor deposition-grown Si-rich SiO₂," *Journal of Applied Physics*, vol. 97, no. 9, Article ID 094306, 8 pages, 2005.
- [32] A. Morales-Sánchez, J. Barreto, C. Domínguez, M. Aceves, Z. Yu, and J. A. Luna López, "Charge trapping and de-trapping in Si-nanoparticles embedded in silicon oxide films," *Physica Status Solidi C*, vol. 5, no. 12, pp. 3651–3654, 2008.
- [33] C. Delerue, G. Allan, and M. Lannoo, "Theoretical aspects of the luminescence of porous silicon," *Physical Review B*, vol. 48, no. 15, pp. 11024–11036, 1993.
- [34] C. Kittel, *Introduction to Solid State Physics*, John Wiley & Sons, New York, NY, USA, 1986.



Hindawi

Submit your manuscripts at
<http://www.hindawi.com>

